

## Supporting Information

### **On-demand continuous H<sub>2</sub> release by methanol dehydrogenation and reforming via photocatalysis in a membrane reactor**

Haimiao Jiao<sup>a</sup>, Jianlong Yang<sup>b</sup>, Xiyi Li<sup>a</sup>, Chao Wang<sup>a</sup> and Junwang Tang<sup>\*a</sup>

<sup>a</sup> Solar Energy and Advanced Materials Research Group, Department of Chemical Engineering, University College London, London, WC1E 7JE, UK.

<sup>b</sup> Key Lab of Synthetic and Natural Functional Molecule Chemistry of Ministry of Education, the Energy and Catalysis Hub, College of Chemistry and Materials Science, Northwest University, Xi'an, P. R. China.

\* Corresponding author at: Solar Energy and Advanced Materials Research Group, Department of Chemical Engineering, University College London, London, WC1E 7JE, UK.

E-mail address: [junwang.tang@ucl.ac.uk](mailto:junwang.tang@ucl.ac.uk) (J. Tang)

## Calculation of apparent quantum efficiency (AQE)

The AQE was measured using the monochromatic light of 365 nm. The detailed calculation step of AQE on 1% Cu/PC50 for photocatalytic methanol dehydrogenation and reforming was shown as follows:

$$\begin{aligned} \text{AQE} &= \frac{2 \times \text{number of generated } H_2 \text{ molecules}}{\text{number of incident photons}} \times 100\% \\ &= \frac{2 \times H_2 \text{ moles/s} \times N_A}{(I \times A)/(E_g \times J)} \times 100\% \\ &= \frac{2 \times \frac{2.95 \times 10^{-6} \text{ mol}}{3600 \text{ s}} \times 6.023 \times 10^{23}}{\left(\frac{0.769 \text{ mW} \times 10^{-3}}{0.785 \text{ cm}^2} \times 3.14 \times (1.5 \text{ cm})^2\right) / (3.40 \text{ eV} \times 1.6 \times 10^{-19})} \times 100\% \\ &= 7.75\% \end{aligned}$$

where  $N_A$  is Avogadro's constant ( $6.02 \times 10^{23}$ ),  $I$  is the measured light intensity (0.980 mW/cm<sup>2</sup>),  $A$  is the light irradiation area (7.065 cm<sup>2</sup>),  $E_g$  is the photon energy at 365 nm wavelength (3.4eV) and  $J$  is the amount of charge in one electron and used to convert the unit of photon energy from eV to J.

## Calculation of selectivity

In this study, the main products were HCHO, HCOOH, CO and CO<sub>2</sub>. Thus, the selectivity (e.g., CO<sub>2</sub>) was calculated as follows:

$$\text{Selectivity}_{CO_2} = \frac{\text{mole}_{CO_2}}{\text{mole}_{CO_2 + CO + HCHO + HCOOH}} \times 100\%$$

## Calculation of turnover frequency (TOF) with respect to Cu

$$\text{TOF (mol}_{H_2}\text{/mol}_{Cu}\text{/h)} = \frac{\text{number of generated } H_2 \text{ molecules}}{\text{number of Cu} \times \text{reaction time}}$$

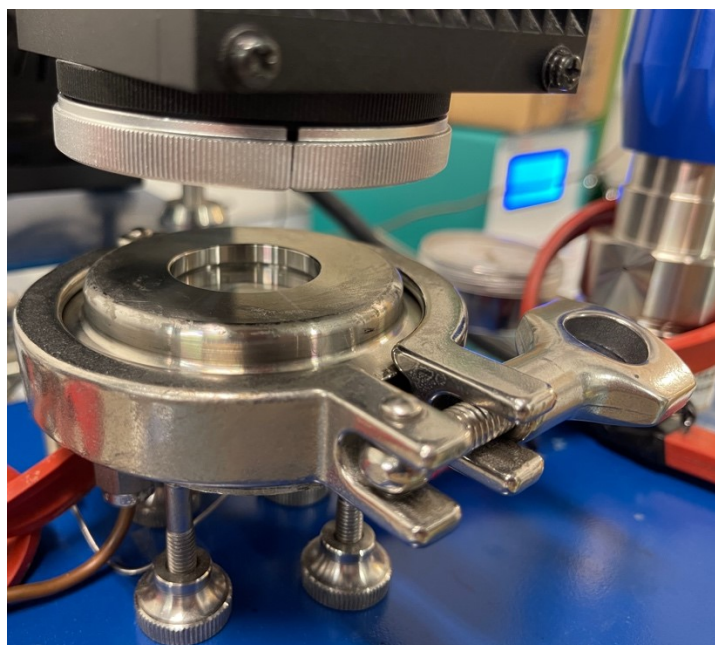


Figure S1. The picture of the flow membrane reactor used for photocatalytic methanol dehydrogenation and reforming.

The custom-designed gastight stainless-steel flow membrane reactor used in this work is provided by Beijing Perfect Light Ltd. One quartz window with a diameter of 3.0 cm is installed at the top of reactor. The photocatalyst-loaded glass fiber membrane is fixed on the porous reactor bed with a diameter of 5.0 cm, which is located at the center of the reactor. A thermal sensor, together with a heater is inserted at the bottom of the reactor bed to monitor and control the reaction temperature. The gaseous reactants are introduced from the bottom of the reactor and pass through the reactor bed and photocatalyst film, then flow into the product collector for the following analysis.

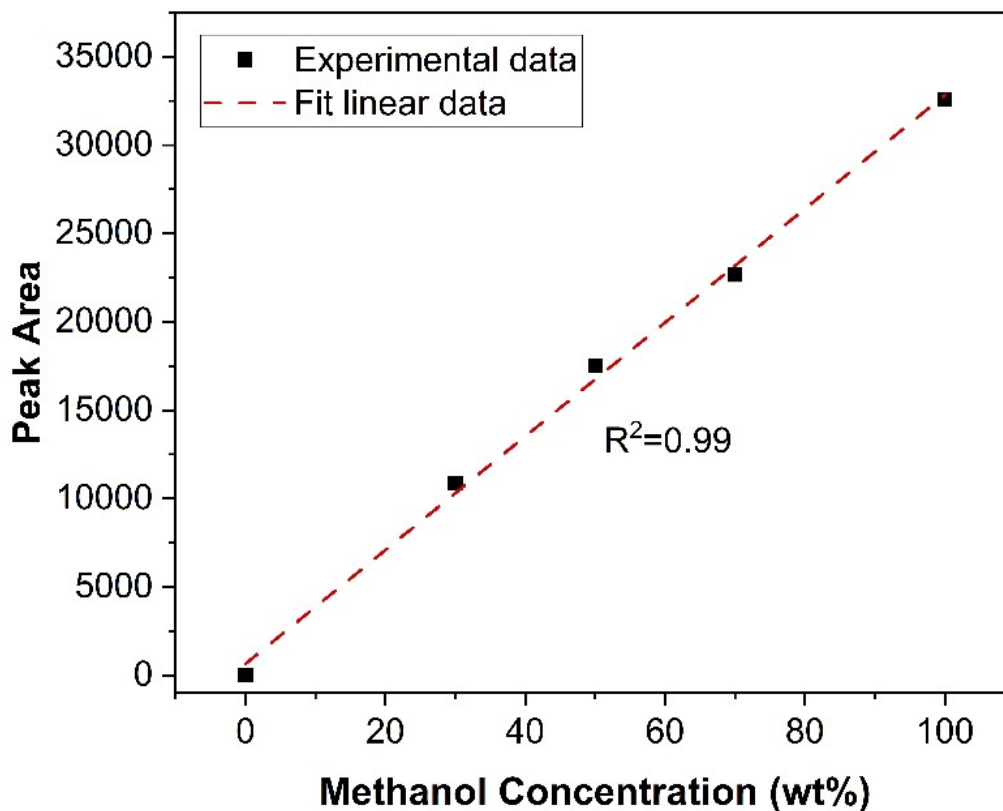


Figure S2. Calibration curve of the standard methanol water solution with methanol concentration (indicated by the peak area) in the headspace of the vial measured by gas chromatography.

In this study, the detailed measurement steps for the methanol concentration in the gas phase at the inlet with different flow rate of argon gas are mentioned follow:

Here we take the measurement of methanol fraction in the gas phase with an argon flow rate of 57.20 ml min<sup>-1</sup> as an example to detail the procedure. First, as the gas chromatography (GC) method is very sensitive to organic substance but cannot analyse water in this study, we had to collect methanol and water vapor at the outlet of the flow membrane reactor within a certain time under the reaction conditions with an argon flow rate of 57.20 ml min<sup>-1</sup> and 50 vol% methanol aqueous solution for subsequent analysis. This was achieved by flowing the gas mixture into one empty vessel merged in a cold trap by liquid nitrogen. Then the gas phase in the headspace of the sealed vessel was analysed by GC.

Second, a series of methanol-water mixture solution with different known methanol concentration were prepared in sealed vials and then analysed by the gas chromatography (GC) to draw a calibration curve. This calibration curve was next used to quantify the corresponding methanol concentration in aqueous phase in the sealed vials. In order to measure the concentration of methanol accurately in the gas phase, all the sealed vials were placed in the water bath with a constant temperature to achieve the gas-liquid equilibrium. Herein, the Raoult's law was used to determine the methanol concentration in aqueous phase.<sup>1</sup> According to the Raoult's law, in a sealed system, when the liquid and gas phase reached thermodynamically equilibrium at a certain temperature and pressure, the concentration of methanol in the liquid solution could be calculated using the corresponding concentration detected in the above gas phase. The standard calibration curve of methanol concentration is shown as Figure S2, which indicates that the GC method is very accurate to know the exact ratio of methanol to water in the liquid solution by analysing the gas phase in the headspace of a vial. Next, we used the measured methanol concentration in the gas phase to calculate the methanol to water ratio in the solution collected in the vial after the membrane reactor.

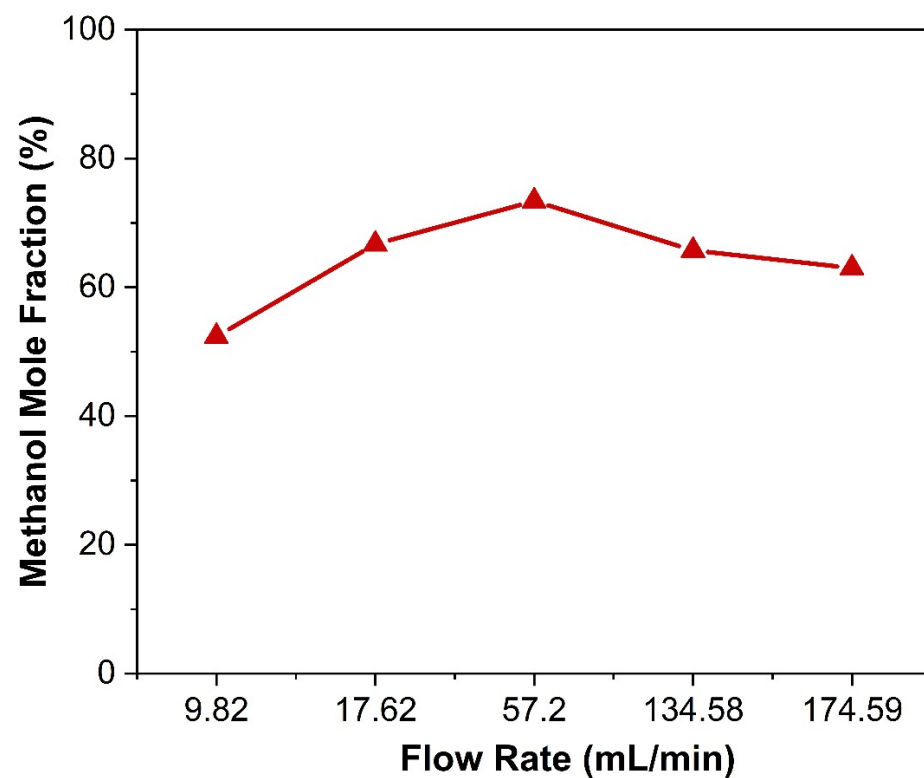


Figure S3. The curve of the measured methanol mole fraction in the methanol-water gaseous mixture at the inlet of membrane reactor with different flow rates of argon gas.

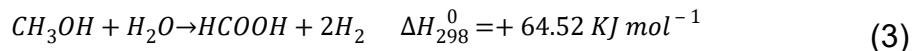
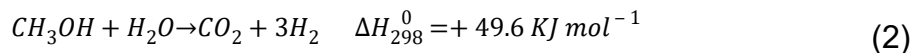
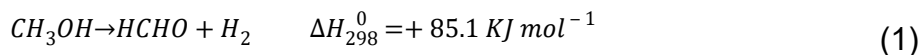
## Calculation of the methanol conversion

To evaluate the accurate methanol conversion in the flow membrane reactor, we used two different methods to obtain this value including the quantitative method by gas chromatography (GC) and the theoretical calculation based on the yield of oxidation products and the details are shown as below.

First, the gas chromatography was used to quantify the methanol concentration at the outlet of the flow membrane reactor before and after light irradiation under the optimal reaction conditions with 50 vol% methanol aqueous solution and an argon flow rate of 57.2 ml min<sup>-1</sup>. With the quantitative measurement, the methanol content in the gas phase at the outlet of membrane reactor before and after light illumination is 3669.38 μmol h<sup>-1</sup> and 3423.51 μmol h<sup>-1</sup>, respectively. As the reduced methanol content represents the consumed methanol which was involved in the photocatalytic dehydrogenation and reforming process, the conversion can be calculated based on the following equation:

$$\begin{aligned} \text{Conversion of methanol (\%)} &= \frac{\text{the consumed methanol content during light irradiation}}{\text{the total methanol content before light irradiation}} \times 100\% \\ &= \frac{3669.38 \mu\text{mol h}^{-1} - 3423.51 \mu\text{mol h}^{-1}}{3669.38 \mu\text{mol h}^{-1}} \times 100\% \\ &= 6.70\% \end{aligned}$$

Besides, the methanol conversion in the flow membrane reactor was also estimated based on the yield of oxidation products. The possible chemical reactions occurred in the flow system would follow the following equations including photocatalytic gaseous methanol dehydrogenation (Eq. 1) and reforming (Eq. 2 and 3):



Assuming all oxidation products were collected properly, based on the yield of produced CO<sub>2</sub> (382.0 μmol g<sup>-1</sup> h<sup>-1</sup>) and HCOOH (264.5 μmol g<sup>-1</sup> h<sup>-1</sup>), the converted methanol rate in the Eq.2 and Eq.3 is determined to be 646.5 μmol g<sup>-1</sup> h<sup>-1</sup>, which is the sum of yield of CO<sub>2</sub> and HCOOH. As the produced H<sub>2</sub> by

the reforming process (Eq. 2 and 3) is around 7% of the total produced H<sub>2</sub>, thus, the converted methanol rate in methanol dehydrogenation process (Eq.1) can be estimated to be 23812 μmol g<sup>-1</sup> h<sup>-1</sup>. Accordingly, the conversion of methanol can be calculated based on the following equation:

$$\begin{aligned}
 \text{Conversion of methanol (\%)} &= \frac{\text{the consumed methanol content during light irradiation}}{\text{the total methanol content before light irradiation}} \times 100\% \\
 &= \frac{(23812 \mu\text{mol g}^{-1} \text{h}^{-1} + 646.5 \mu\text{mol g}^{-1} \text{h}^{-1}) \times 0.01 \text{ g}}{3669.38 \mu\text{mol h}^{-1}} \times 100\% \\
 &= 6.67\%
 \end{aligned}$$

According to the above results, one can see that the methanol conversion estimated by two different methods are quite close. Thus, we can conclude that the methanol conversion rate in the flow membrane reactor is 6.7%.



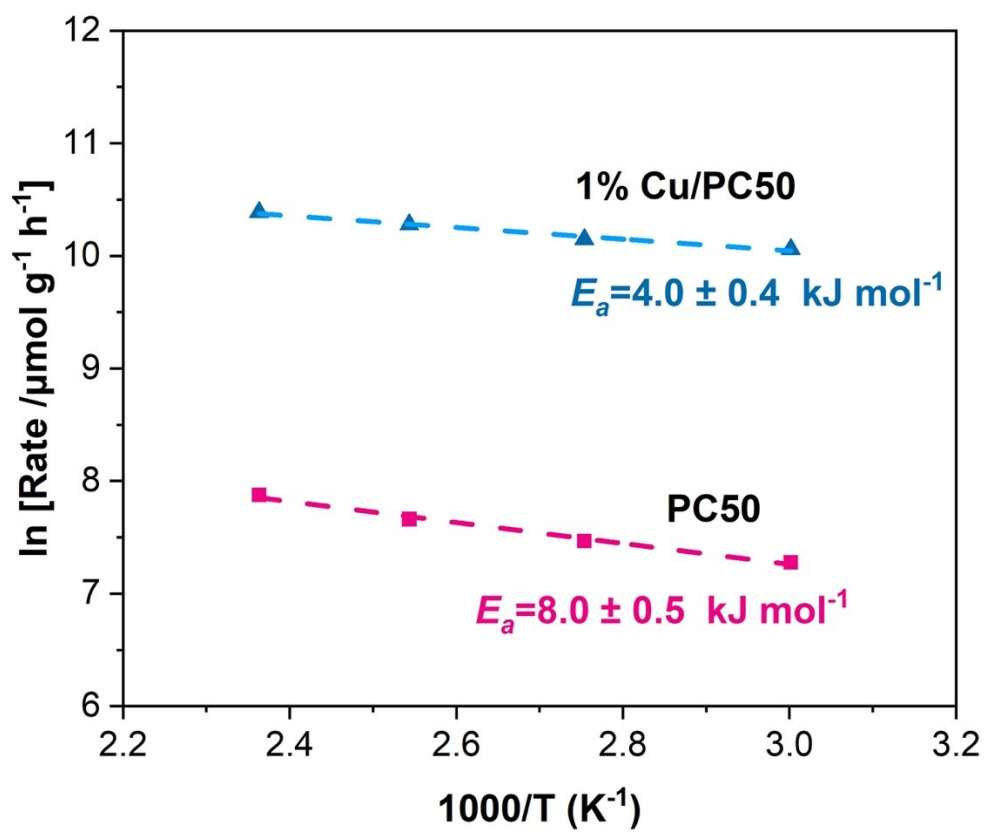


Figure S4. Apparent activation energies  $E_a$  of 1% Cu/PC50 and PC50.

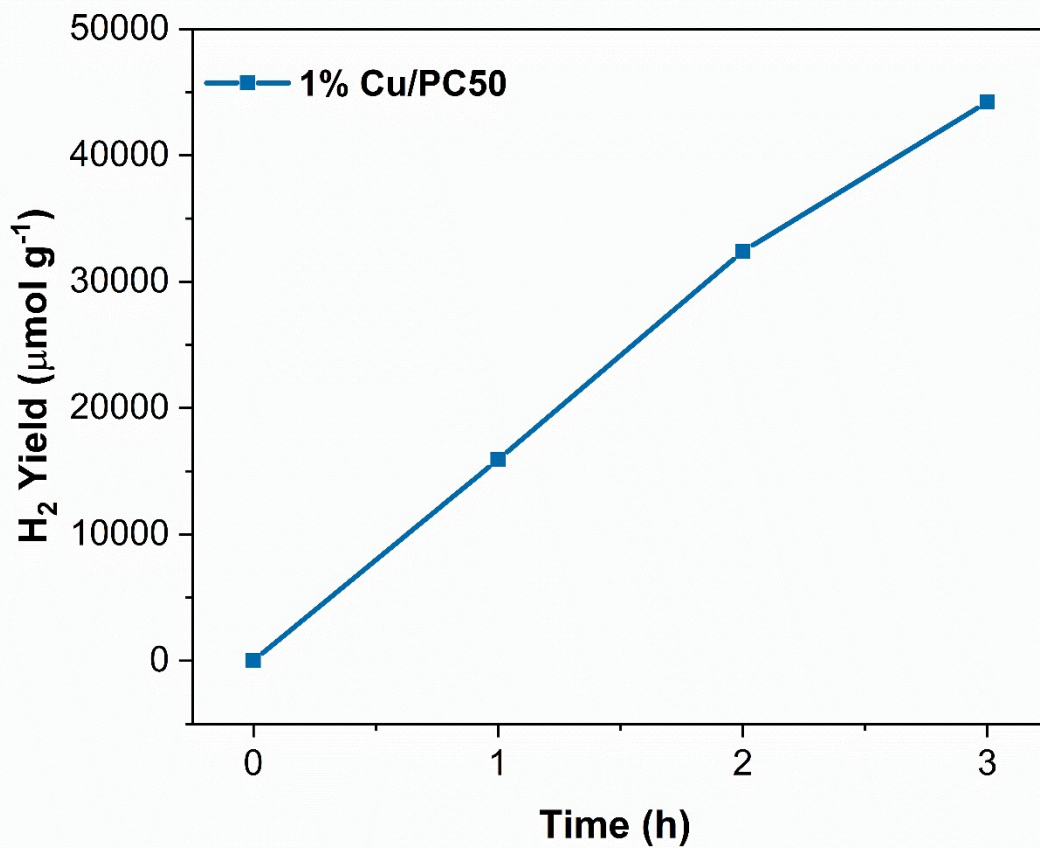


Figure S5. The yield of H<sub>2</sub> on 1% Cu/PC50 in a batch reactor with 50 vol% methanol aqueous solution.

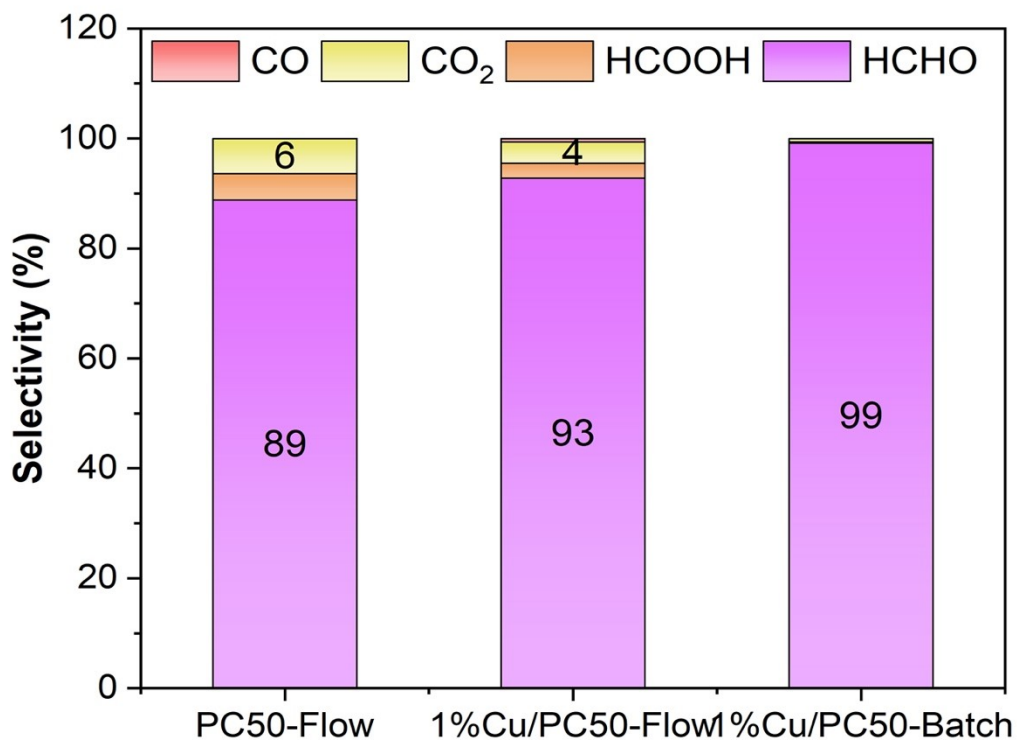


Figure S6. Comparison of the selectivity of C1 products in the photocatalytic methanol dehydrogenation and reforming over PC50 and 1% Cu/PC50 in the flow and batch system.

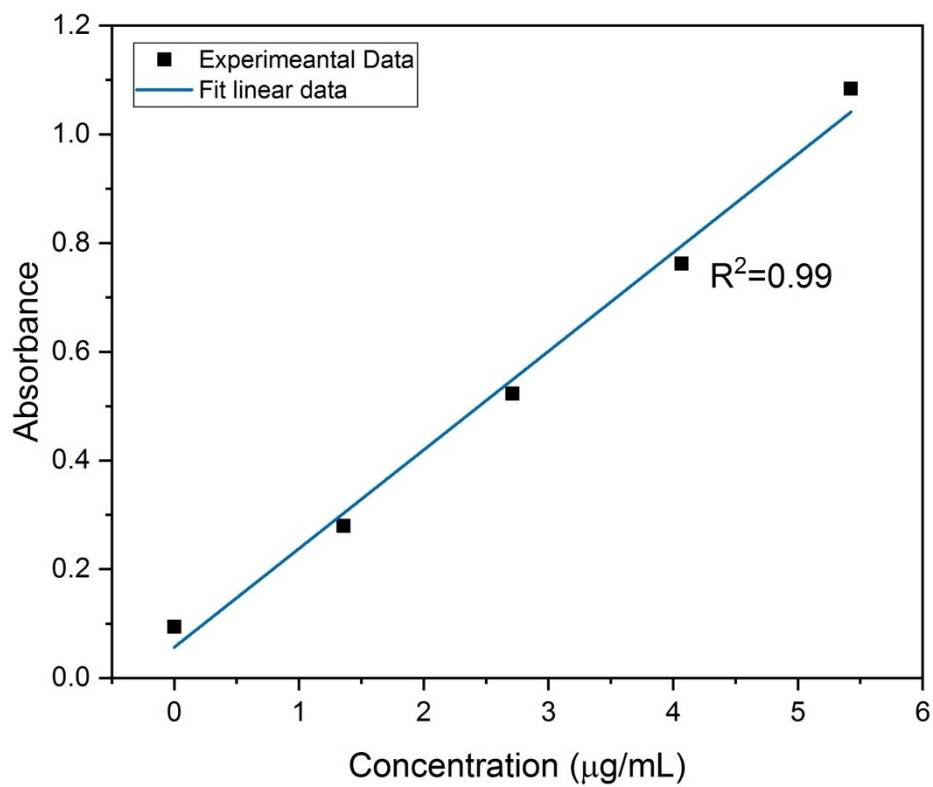


Figure S7. Standard calibration curve of the formaldehyde by colorimetric method.

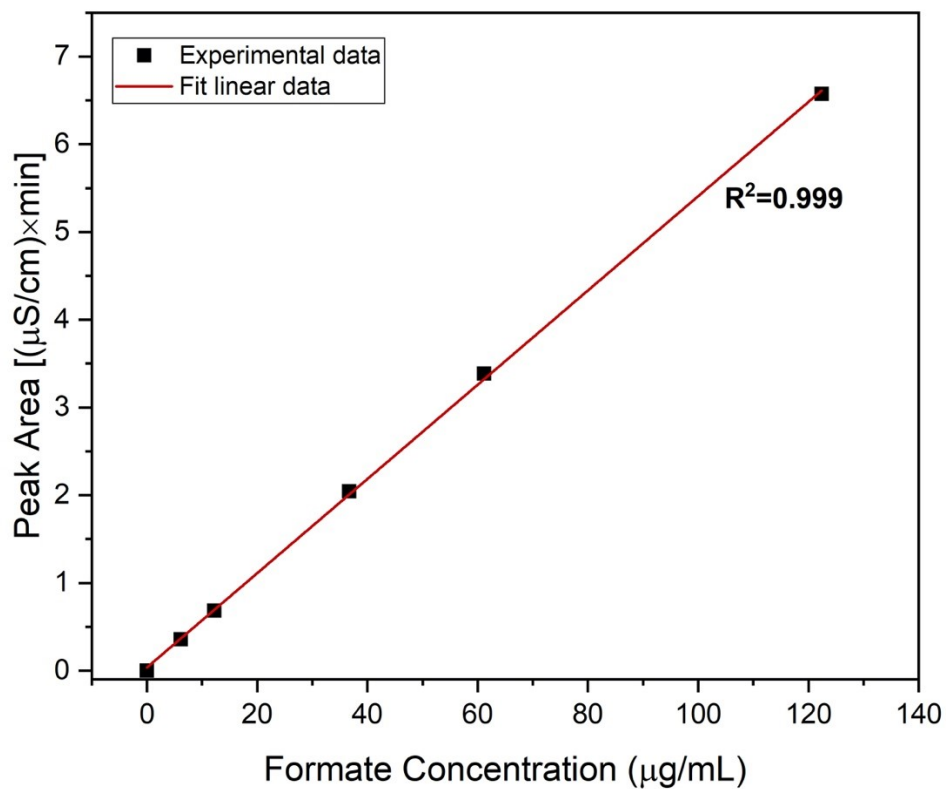


Figure S8. Standard calibration curve of the formate ion by ion chromatography.

Table S1. Comparison of performance for H<sub>2</sub> production from methanol in different photocatalytic systems

Catalyst	Reactor Type	Reactants	Light Source	Temperature of reactor (K)	H <sub>2</sub> yield ( $\mu\text{mol g}^{-1} \text{h}^{-1}$ )	Ref
1 wt% Cu <sub>x</sub> O/PC50	Flow	Methanol, H <sub>2</sub> O	300 W Xe Lamp	303, 333	25487, 33702	This work
1 wt% Pt/P25	Flow	Methanol, H <sub>2</sub> O	Hg Lamp	303	18600	2
1 wt% Au/FP-TiO <sub>2</sub>	Flow	Methanol, H <sub>2</sub> O	Hg Lamp	303	10200	3
Rh/TiO <sub>2</sub>	Flow	Methanol, H <sub>2</sub> O	Xe lamp	483	15000	4
MgO	Slurry	Methanol	Hg Lamp	298	320	5
Ag/g-C <sub>3</sub> N <sub>4</sub>	Slurry	Methanol	300 W Xe Lamp	298	152	6
MoS <sub>2</sub>	Slurry	Methanol	AM 1.5	298	617	7
Ni <sub>2</sub> P/CdS	Slurry	Methanol	300 W Xe Lamp ( $\lambda > 420 \text{ nm}$ )	298	580	8
Ni/CdS	Slurry	Methanol	300 W Xe Lamp ( $\lambda > 420 \text{ nm}$ )	298	7700	9
MoS <sub>2</sub> foam/CdS	Slurry	Methanol, H <sub>2</sub> O	300 W Xe Lamp ( $\lambda > 420 \text{ nm}$ )	298	12000	10

NiAu/TiO <sub>2</sub>	Slurry	Methanol, H <sub>2</sub> O	Hg Lamp	298	3140	11
Cu/TiO <sub>2</sub>	Slurry	Methanol	300 W Xe Lamp	298	19200	12
0.75 wt% Cu/TiO <sub>2</sub>	Slurry	Methanol, H <sub>2</sub> O	300 W Xe Lamp	298	16600	13
0.6 wt% Pt/black hydrogenat ed TiO <sub>2</sub>	Slurry	Methanol, H <sub>2</sub> O	AM 1.5	298	10000	14

Table S2. Real percentage of Cu over TiO<sub>2</sub> detected by ICP-AES

	Cu/TiO <sub>2</sub> (wt. %)
--	-----------------------------

Sample	Designed	Detected (ICP-AES)
0.05% Cu/TiO <sub>2</sub>	0.05	0.04
0.1% Cu/TiO <sub>2</sub>	0.1	0.09
0.5% Cu/TiO <sub>2</sub>	0.5	0.52
1% Cu/TiO <sub>2</sub>	1	0.95
2% Cu/TiO <sub>2</sub>	2	1.53



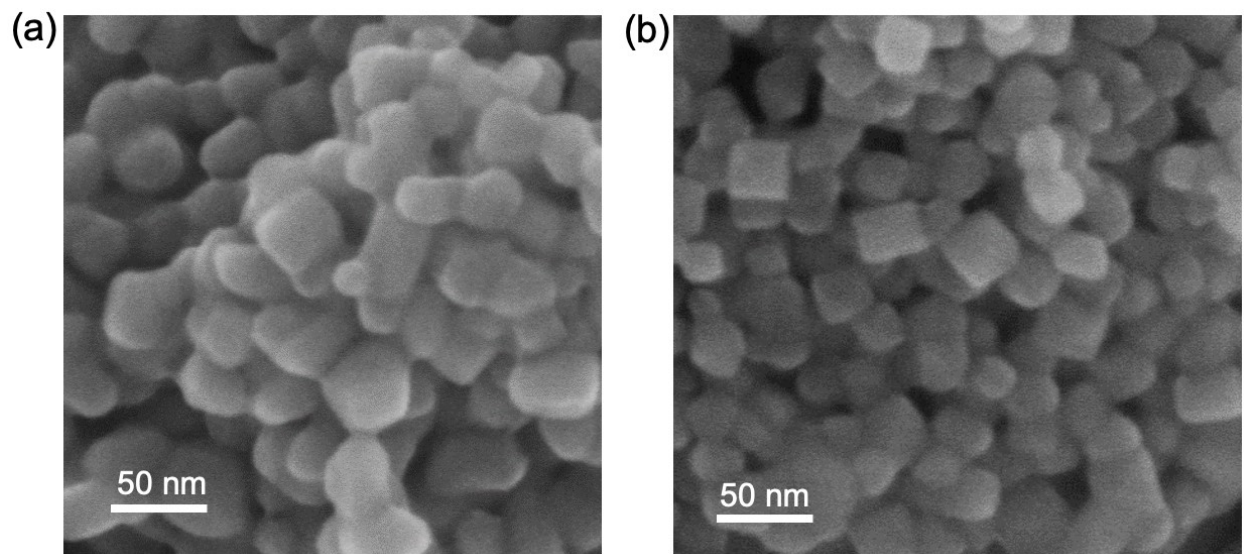


Figure S9. SEM images of (a) PC50 and (b) 1% Cu/PC50.

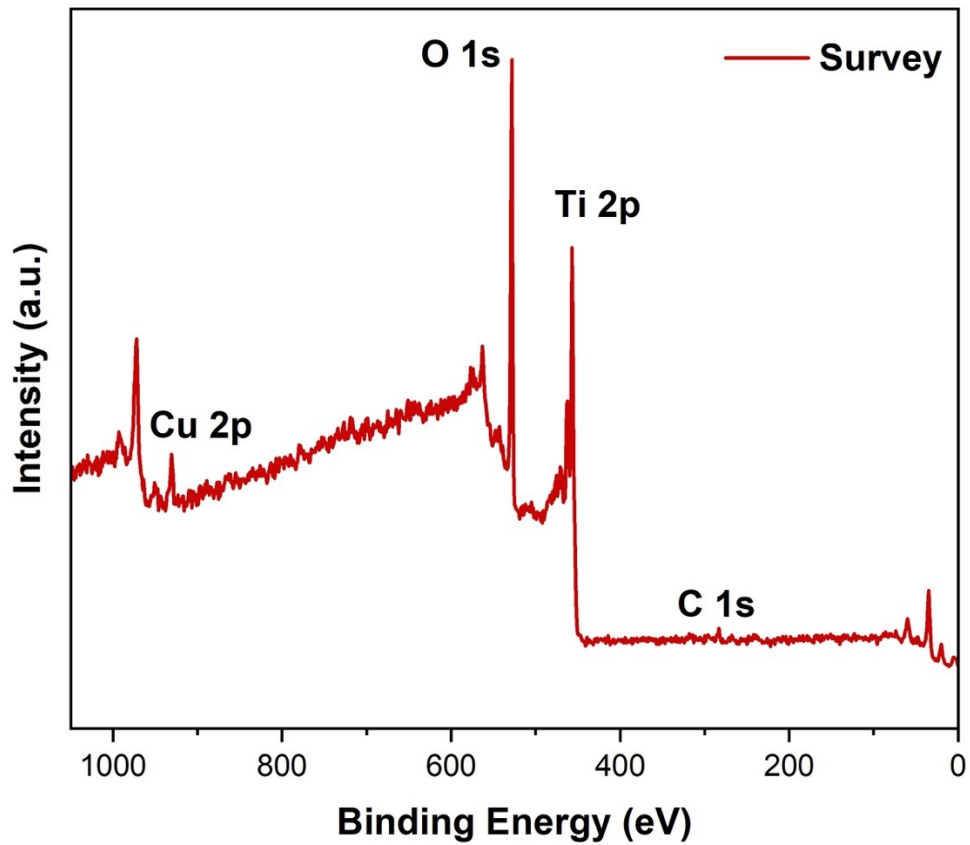


Figure S10. XPS survey spectrum of 1% Cu/TiO<sub>2</sub> in the dark condition.

## References

1. J. Xie, R. Jin, A. Li, Y. Bi, Q. Ruan, Y. Deng, Y. Zhang, S. Yao, G. Sankar, D. Ma and J. Tang, *Nat. Catal.*, 2018, **1**, 889-896.
2. G. L. Chiarello, M. H. Aguirre and E. Selli, *J. Catal.*, 2010, **273**, 182-190.
3. G. L. Chiarello, L. Forni and E. Selli, *Catal. Today*, 2009, **144**, 69-74.
4. S. Fang, Y. Liu, Z. Sun, J. Lang, C. Bao and Y. H. Hu, *Appl. Catal. B: Environ.*, 2020, **278**, 119316.
5. Z. Liu, Z. Yin, C. Cox, M. Bosman, X. Qian, N. Li, H. Zhao, Y. Du, J. Li and G. Nocera Daniel, *Sci. Adv.*, **2**, e1501425.
6. Y. Liu, S. Yang, S.-N. Yin, L. Feng, Y. Zang and H. Xue, *Chem. Eng. J.*, 2018, **334**, 2401-2407.
7. Y. Pang, M. N. Uddin, W. Chen, S. Javaid, E. Barker, Y. Li, A. Suvorova, M. Saunders, Z. Yin and G. Jia, *Adv. Mater.*, 2019, **31**, 1905540.
8. Y. Chao, J. Lai, Y. Yang, P. Zhou, Y. Zhang, Z. Mu, S. Li, J. Zheng, Z. Zhu and Y. Tan, *Catal. Sci. Technol.*, 2018, **8**, 3372-3378.
9. Z. Chai, T.-T. Zeng, Q. Li, L.-Q. Lu, W.-J. Xiao and D. Xu, *J. Am. Chem. Soc.*, 2016, **138**, 10128-10131.
10. S. Xie, Z. Shen, J. Deng, P. Guo, Q. Zhang, H. Zhang, C. Ma, Z. Jiang, J. Cheng, D. Deng and Y. Wang, *Nat. Commun.*, 2018, **9**, 1181.
11. A. L. Luna, E. Novoseltceva, E. Louarn, P. Beaunier, E. Kowalska, B. Ohtani, M. A. Valenzuela, H. Remita and C. Colbeau-Justin, *Appl. Catal. B: Environ.*, 2016, **191**, 18-28.
12. F. Yu, L. Chen, X. Li, X. Shen, H. Zhao, C. Duan and Q. Chen, *ACS Appl. Mater. Interfaces*, 2021, **13**, 18619-18626.
13. B.-H. Lee, S. Park, M. Kim, A. K. Sinha, S. C. Lee, E. Jung, W. J. Chang, K.-S. Lee, J. H. Kim, S.-P. Cho, H. Kim, K. T. Nam and T. Hyeon, *Nat. Mater.*, 2019, **18**, 620-626.
14. X. Chen, L. Liu, Y. Yu Peter and S. Mao Samuel, *Science*, 2011, **331**, 746-750.